Worst case climate simulations show that heatwaves could cause major disruptions in the Paris 2024 Olympics

Pascal Yiou, Camille Cadiou, Davide Faranda, Aglaé Jézéquel, Nemo Malhomme, George Miloshevich, Robin Noyelle, Flavio Pons, Yoann Robin, Mathieu Vrac

Worst case climate simulations show that heatwaves could cause major disruptions in the Paris 2024 Olympics

Pascal Yiou[1*], Camille Cadiou[1], Davide Faranda[1,2,3], Aglaé Jézéquel[3,4], Nemo Malhomme[1], George Miloshevich[1], Robin Noyelle[1], Flavio Pons[1], Yoann Robin[1] and Mathieu Vrac[1]

[1*]Laboratoire des Sciences du Climat et de l'Environnement, UMR 8212 CEA-CNRS-UVSQ, IPSL & U Paris-Saclay, CE Orme des Merisiers, Gif-sur-Yvette, 91191, France.
[2]London Mathematical Laboratory, 8 Margravine Garden, London, W6 8RH, UK.
[3]Laboratoire de Météorologie Dynamique, UMR CNRS-ENS-X, 24 rue Lhomond, Paris, 75005, France.
[4]Ecole des Ponts Paristech, Champs-sur-Marne, 77420, France.

*Corresponding author(s). E-mail(s): pascal.yiou@lsce.ipsl.fr.fr;

Abstract

The Summer Olympic Games in 2024 will take place during the apex of the temperature seasonal cycle in the Paris Area. The midlatitudes of the Northern hemisphere have witnessed a few intense heatwaves since the 2003 event [1]. Those heatwaves have had environmental and health impacts, which often came as surprises [2]. In this paper, we search for the most extreme heatwaves in Ile-de-France that are physically plausible, under climate change scenarios, for the decades around 2024. We circumvent the sampling limitation by applying a rare event algorithm [3] on CMIP6 data [4] to evaluate the range of such extremes. We find that the 2003 record can be exceeded by more than **4**°C in Ile-de-France before 2050, with a combination of prevailing anticyclonic conditions and cut-off lows. This study intends to build awareness on those unprecedented events, against which our societies are ill-prepared. Those results could be extended to other areas of the world.

Keywords: Climate change, Rare events, Extreme Heatwaves

1 Introduction

Summer heatwaves in the northern midlatitudes have lead to many impacts on society and ecosystems, since the major event that struck Western Europe in 2003 [1]. Since that epitome event, nations have taken measures to mitigate the effects of such extremes, especially on public health [5] and energy [6]. Climate model projections have suggested that the records of the early 21st century could be regularly broken in the second part of the 21st century [7].

The Olympic games in 2024 will take place in Paris between July 26th and August 10th, which is at the apex of the temperature seasonal cycle. During that event, it is expected that tens of thousands of visitors from the whole world will stay outdoors, and be exposed to potential heat stress. As shown in Figure 1a, the preceding summer Olympics in Tokyo (2021) were the warmest on the record since 1952, with an average temperature that exceeded the value in Paris in 2003. The Tokyo heatwave had huge impacts on the athletes and volunteers during outdoor competitions [8]. Health impacts on the public had been anticipated [9, 10], but the COVID crisis limited the foreign public exposure in 2021.

Anticipating the risks of an intense heatwave in the present decades, i.e. a worst case scenario, is crucial for society. The field of Extreme Event Attribution (EEA [11]) has built concepts and methods to evaluate if and how climate change has altered the probabilities of extreme events. Many of the results of EEA rely on ensembles of physical or statistical model simulations. A recently developed approach to gain numerical efficiency has applied rare event algorithms [12] that nudge trajectories towards extreme values. This approach allows simulating the most extreme events, without having to consider most "normal" events. So far, this approach has been based on single model experiments [12, 13] or constrained by reanalysis data [3]. Both studies focused on present-day or pre-industrial conditions. Therefore there is an urge to be able to apply this type of methods to scenarios of climate change, in order to evaluate worst cases in near future climate conditions.

We consider mean daily temperature (TG) and we determine the warmest period of 15 days (in Ile-de-France) in July-August, for each year (TG15d). This length (15 days) is motivated by the duration of Olympic games. The goal of this paper is to estimate worst case scenarios of TG15d heatwaves in the Paris area in the decades around 2024, and outline the synoptic features of those events in order to understand whether their causes are unique. The strategy is to use a stochastic model constrained by the atmospheric circulation [14, 15] to simulate large ensembles of extreme heatwaves that are consistent with state-of-the-art climate models. This stochastic model will consider four scenarios for climate change (SSP1-2.6, SSP2-4.5, SSP3-7.0, SSP5-8.5) and a panel of coupled climate model simulations as input (see Section 3.5). We use a set of 14 CMIP6 model simulations [4] to sample the model dependence of the simulation of extreme heatwaves. A state-of-the-art bias correction method [16] is applied, so that the main statistics of the present-day model simulations are close to observations. In order to build robustness, a statistical analysis of extremes [17] allows estimating the probabilities of extreme events, and their dependence on the emission scenarios. The methods and data are described in the Methods section 3.

2 Results

Temperature time series of the warmest 15-day periods (TG15d) in July-August in Ile-de-France are shown in Figure 1a, for the IPSL climate model (one simulation for each scenario). As anticipated by the bias correction procedure, the temperature variability is similar to the ERA5 reanalysis [18] variability for all models (Figure 1a, b). In the IPSL model, the July-August average summer temperature increases by ≈1.6 to ≈ 2.1°C from 1951-2000 to 2001-2050, depending on the scenario. The average TG15d increases by ≈1.4 to ≈ 2.2°C (Figure 1a) over the same period, depending on the SSP scenario. The differences of the maximum of TG15d between those two periods range from 1.8 to 3.5 °C in the IPSL model, depending on the scenario. The largest difference is obtained for SSP2-4.5. Therefore, the mean July-August and TG15d show a similar mean increase, while the maximum values of TG15d yield a larger increase for this model.

We summarize the variability range of TG15d in CMIP6 simulations in Figure 1b. This illustrates the most extreme values that can be reached with this multi-model ensemble, under the four SSP scenarios. This shows that bias corrected CMIP6 simulations sample the variability of temperature obtained by ERA5 reanalysis in the historical period. A Kolmogorov-Smirnov test cannot detect differences between the empirical probability distributions of TG15d in four CMIP6 SSP scenario simulations between 2001 and 2050. The most extreme values of TG15d in 2001-2050 (in CMIP6 data) are not necessarily detected in SSP5-8.5 simulations, because the scenario simulations are barely distinguishable before 2050. The observed record value (in ERA5) for the summer warmest 15 days in 2003 (26.8 °C) is never exceeded in the 20th century in CMIP6 simulations (green boxplots in Figure 1b), and is occasionally exceeded (less than 10% time) in 2001-2050. This plot motivates the simulation of events that are close to the upper limit of those known values (Figure 1b), as the mean temperature increase (over the whole season or TG15d) between 1951-2000 and 2001-2050 is likely to increase the probability of breaking the 2003 record.

For comparison purposes, we report the 15 day average temperatures during the summer Olympic games since 1952 at each organizing city (nearest gridpoint in ERA5, triangles in Figure 1a). The Olympic games were organized at different periods of the year and different hemispheres, but the temperatures yield a general increasing trend. Only the last Olympics in Tokyo (23 July 2021 to 8 August 2021) had a temperature that exceeded the French record in 2003, but had a limited number of attendants due to the COVID-19 crisis, which lowered the exposure of vulnerable persons to extreme heat.

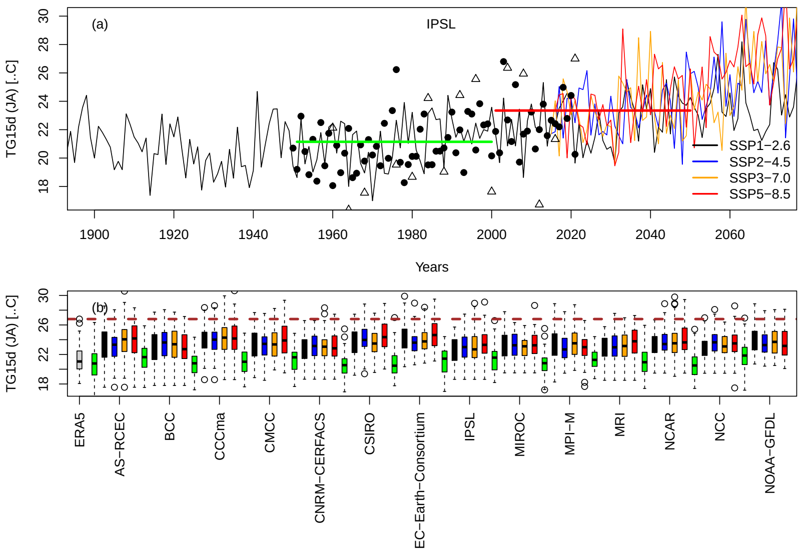

Fig. 1 Panel a: Time series of Ile-de-France temperature. The values correspond to the July-August maximum of moving 15 day averages (TG15d) in IPSL model simulations with four SSP scenarios. The black line is for the historical period (1900-2014). The colored lines are for the scenarios (2015-2100). The circles represent temperature variations in the ERA5 reanalysis. The triangles represent the 15-day average temperature during the preceding Olympics, in each organizing city, since 1952 (the temperatures during the summer Olympics in 1952 and 1956 were lower than 15°C). The two horizontal bars represent the average over the two key periods (1951-2000: green; 2001-2050: red for SSP5-8.5). Panel b: boxplots of maximum 15 day temperature over Ile-de-France for each model and each SSP scenario. The grey boxplot on the left is for ERA5 (1950-2021). Green boxplots are for 1951-2000. black, blue, orange and red boxplots are for 2001-2050, with the SSP1-2.6, SSP2-4.5, SSP3-7.0 and SSP5-8.5 scenarios, respectively. The horizontal brown dashed line is the 2003 value (TG15d= 26.8° C) in ERA5. Boxplots show the 25th (q25), median (q50) and 75th (q75) quantiles of the distribution (boxes). The upper whisker is classically: $\min\{1.5 \times (q75 - q25) + q50, \max(\mathrm{TG15d})\}$. The lower whiskers are the symmetric expressions for lower values. The circles above (or below) the whiskers are the values larger (or smaller) than 1.5 times the interquartile range.

We illustrate the SWG simulations of extreme events with data from the IPSL model with four SSP scenarios. We compare 15-day SWG simulations starting the first day of the TG15d identified in Figure 1a in 2001-2050. Therefore, the initial conditions depend on the years because TG15d can occur between the 1st of July and the 31st of August, and the SSP scenarios. Hence we show how the extremes simulated with the SWG depend on the reference period of analogs (1951-2000 vs. 2001-2050).

The probability distribution of all TG15d values slightly changes with SSP scenarios (similar medians and non significant Kolmogorov-Smirnov tests on the horizontal lines in Figure 2). The record 2003 value is exceeded in the three "intense" SSP scenarios, although not in SSP1-2.6, with this IPSL model simulation. The highest values for TG15d can occur with any scenario, when considering the CMIP6 ensemble (not shown).

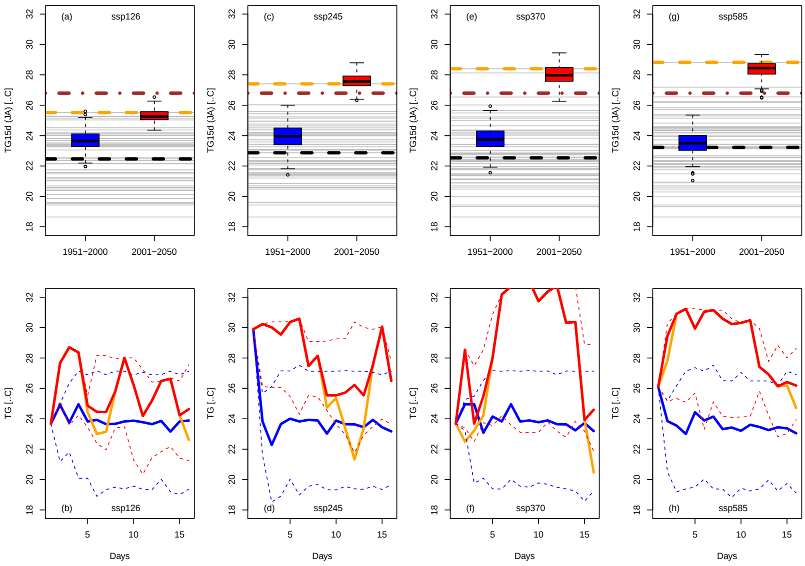

Fig. 2 Upper panels (a, c, e, g): Boxplots of 200 SWG simulated mean 15 day temperatures, with analogues in 1951-2000 (blue) and 2001-2050 (red) in the IPSL model data for the four SSP scenarios (see Methods Section on simulation protocol). The reported SWG simulations start on the initial condition of the warmest TG15d identified in 2001-2050 (orange horizontal dashed line) from each IPSL model simulation. Each panel is for an SSP simulation. Horizontal lines represent TG15d in each IPSL model SSP simulation (obtained from Figure 1a). The dashed black line is the median, for each SSP simulation. The horizontal brown dash dotted line is the value that was observed in 2003, from ERA5 (Figure 1a). Lower panels (b, d, f, h): time variations of the simulated temperatures with the SWG. The blue lines are for SWG simulations with analogs in 1951-2000. The red lines are for SWG simulations with analogs in 2001-2050. The thick continuous lines represent the median of 200 simulations. The dashed lines are the daily 5th and 95th quantiles of the 200 simulations. The thick orange lines are the daily variations for the record year identified in the upper panels. The temperature range for daily variations sometimes exceeds 32°C (panel g) and is close to the 95th quantile most of the time. Daily mean temperatures can exceed 32°C for SSP3-7.0 (panel (f)).

This results with SWG simulations from the IPSL model data (boxplots in Figure 2a–d) show that the temperature increase of the most extreme events between 1951-2000 and 2001-2050 exceeds 3.5 °C in three SSP scenario simulations. The SWG heatwaves with analogs in 1951-2000 span the upper half of the TG15d values in 2001-2050, but not the outliers (Figure 2). The value observed in 2003 (in ERA5) is not reached with SWG simulations from the IPSL model and analogs in 1951-2000. The 2003 observed record (red dash-dotted lines in Figure 2) is exceeded by a large margin in SSP2-4.5, SSP3-7.0 and SSP5-8.5 scenarios (orange lines vs. brown lines in Figure 2), between 2040 and 2050, although it is still a rare value in 2001-2050. The most intense TG15d heatwaves detected in the IPSL model data (orange dashed lines) can be exceeded by 1 °C or with probability that exceeds 20% (upper whiskers in Figure 2) with the SWG simulations and analogs in 2001-2050. The occurrence of a heatwave that exceeds the 2003 record value (red dash-dotted lines) by almost 2 °C in the 2001-2050 is possible, except in the SSP1-2.6 scenario.

Daily time series of simulated temperatures with SWG are shown in the lower panels of Figure 2. The simulations with analogs in 1951-2000 yield a larger temporal variability, as shown by the 90% confidence intervals. The initial conditions are chosen in 2001-2050 for all SWG simulations. This explains why the simulations with analogs in 1951-2000 sometimes decrease after the second day (e.g. in SSP2-4.5 and SSP5-8.5). The simulations with analogs in 2001-2051 mostly stick to the upper quantile, leading to a lower variance.

We investigate the atmospheric circulation patterns during the 15-day heatwaves, for the IPSL model. Figure 3 (first column) shows the 15-day average of SLP and SLP anomalies during the most extreme heatwaves in 2001-2050 detected in each scenario simulation. The four identified extreme heatwaves occur between 2033 (SSP5-8.5) and 2049 (SSP2-4.5). As expected from other studies [19, 20], the four record heatwaves are characterized by strong anticyclonic conditions over Scandinavia and west of France. A cyclonic SLP anomaly is detected over France, which is reminiscent of a cut-off low that advects warm air into France from North Africa. As was observed in the summer 2022, this combination of general anticyclonic conditions and a cut-off low contributes to temperature increases in the summer. The stochastic simulations with analogs in 1951-2000 (Figure 3, central column) exhibit very similar circulation patterns, with this combination of anticyclonic conditions and a cut-off low. The stochastic simulations with analogs in 2001-2050 (Figure 3, right column) are very similar to the record events (left column) because the simulations can select analogs during those events.

The similarities of the atmospheric patterns over the North Atlantic during the most extreme heatwaves across the four SSP scenarios (in one model) suggest that "ultimate" heatwaves that are likely to strike Ile-de-France are associated with this combination of an extended blocking (which can last for several weeks) leading to clear skies and low winds, and a cut-off low (whose lifetime is just a few days) that pumps warm air into Europe. The heatwaves that occurred in France in the 21st century are examples of this combination.

The SWG simulations are applied to other CMIP6 simulations, to test the robustness of the results reported in Figure 2 and the IPSL model. The procedure is the same as for the IPSL model (see Methods).

There is a large variability of extreme heatwave simulations across CMIP6 models (Figure 4). The value of extremes often increases by more than 4 °C between 1951-2000 and 2001-2050. The value of the 2003 observed record is reached only once (MIROC) with the analogs in 1951-2000, and starting with an initial condition in 2001-2050. The MIROC model is the only one for which the record value of 26.8°C (observed in 2003 in ERA5) is almost reached in the historical period (26.6° in 1984 in the MIROC calendar). The initial condition leading to the record in 2001-2050 (in 2043 for SSP5-8.5) is similar to the initial condition leading to the record in 1984, in the MIROC model years.

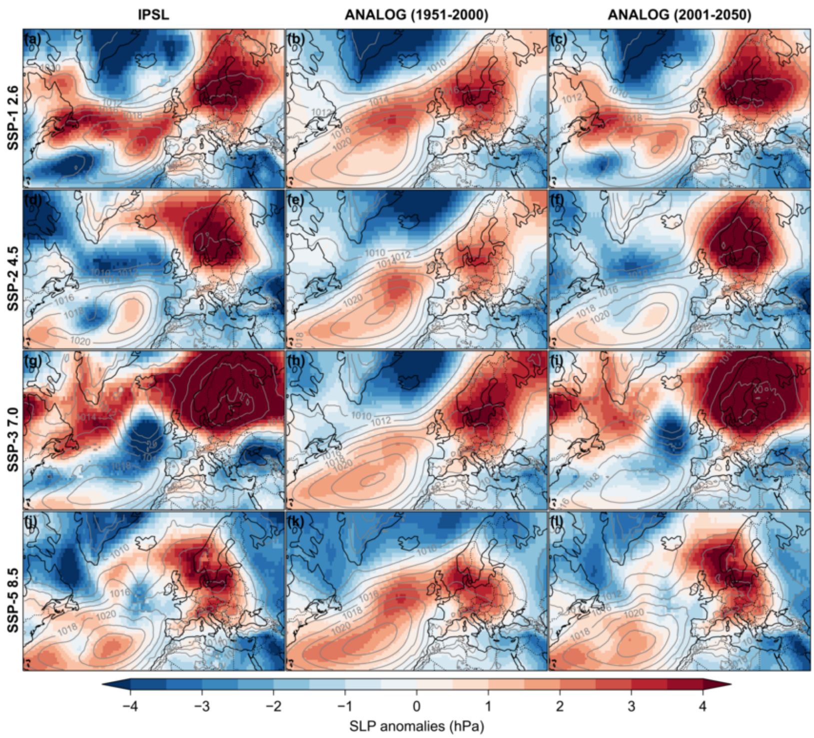

Fig. 3 SLP maps over the North Atlantic region during 15 day heatwaves detected in four IPSL ssp simulations (left panels a, d, g, j). Extreme simulations with analogs in 1951-2000 (central panels b, e, h, k). Extreme simulations with analogs in 2001-2050 (right panels c, f, i, l). Colors represent SLP anomalies (hPa). Isolines represent SLP (hPa).

This explains the apparent outlier of the temperature distribution for SSP5-8.5 with the MIROC model (Figure 4d). The 2003 value (of ERA5) is exceeded for most models in 2001-2050, for all initial conditions.

The mean and median temperatures of average 15-day temperature marginally increase with the SSP scenario (Figure 1b). Likewise, the most extreme values that are simulated by the SWG only slightly increase from SSP1-2.6 to SSP5-8.5, when pooling all models together, from 23.6°C to 24°C. This increase is smaller than the intermodel standard deviation ($\approx$ 1.2°C). Some models allow simulating the highest TG15d from "weaker" SSP scenarios (e.g., CMCC, EC-Earth). This is due to the fact that those model simulations (with SSP1-2.6) yield record shattering TG15d events, which exceed the values obtained in 2001-2050 for the other scenarios.

The SLP maps of CMIP6 simulations are shown in the Supplementary Information. With few exceptions, the circulation scenario that was described for the IPSL model can be applied to the CMIP6 ensemble (see figures in the supplementary information).

We compare those simulations results with a multi-model estimate of extreme values of temperature (see Methods in Section 3). Most CMIP6 models

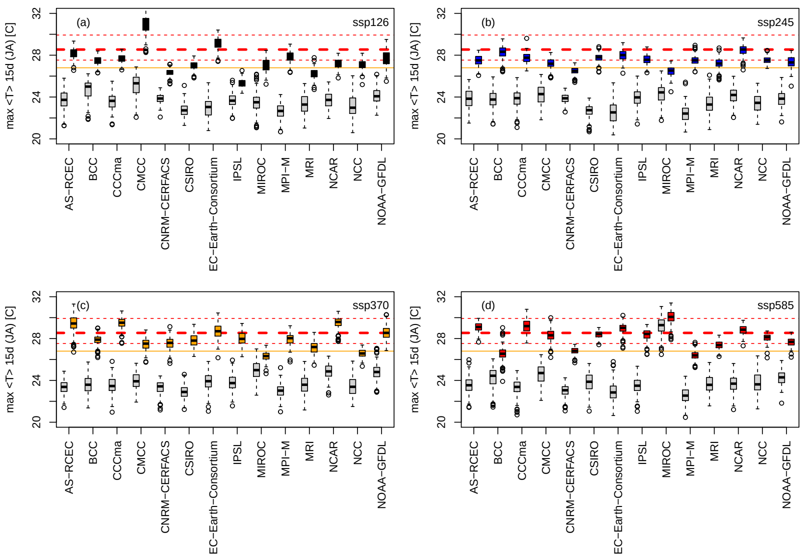

Fig. 4 Boxplots of maximum 15 day averages, starting on the most extreme heatwave in 2001-2050, detected in each CMIP simulation. Panels are for the four ssp scenarios. Grey boxplots are for analogs in 1951-2000. Colored boxplots are for analogs in 2001-2050. Thick horizontal red lines represent estimates of return levels with a return period of 100 years, with a multi-model Generalized Extreme Value (GEV) estimate (see Methods section). The dashed horizontal red lines represent the 95% confidence interval of the return value estimates. Orange horizontal lines represent the value in 2003 from the ERA5 reanalysis.

provide estimates that are close to Generalized Extreme Value (GEV) return levels (red lines, see Methods section) with a return period of 100 years. A few CMIP6 models exceed the GEV upper estimate by almost 1 °C.

3 Methods

3.1 Data and bias correction

We use the simulations of 14 CMIP6 models (out of 31 models) [4] (see Table 1 in the SI) and four shared socio-economic pathways (SSP) scenarios [21] (SSP1-2.6, 2-4.5, 3-7.0 and 5-8.5). The criterion to retain these models is their availability on an ESGF server for the four SSP scenarios on daily increments. A data quality check is also performed on the available files. The historical simulations cover 1850-2014. The scenario (SSP) simulations cover 2015-2100. We extract the model gridpoints that cover continental France. For simplicity, we take one simulation for each model (some models provide ensembles) and visually check that this choice samples the overall spread of all simulations.

The multivariate bias correction method R^2D^2 [16] is used to correct the bias of the marginals and the dependency structure of the temperature and precipitation, with respect to the SAFRAN reanalysis [22] (≈ 8km of horizontal resolution). The R^2D^2 method is based on the CDF-t method [23], which takes into account of the climate change signal. The method is trained on the 1976-2005 period, and applied between 1850 and 2100 on moving periods of 10 years.

We compute the spatial average of the mean daily temperature over Ile-de-France. The 2001-2050 decades stand across the historical and scenario range. We aggregate the historical (1850-2014) and scenario (2015-2100) simulations, to obtain $4 \times 14 = 56$ time series of daily temperatures.

Circulation analogs are computed from SLP fields from the same models over the North Atlantic region. Other fields (e.g. geopotential height at 500hPa) could be used in principle, but only SLP is available on a daily basis for the 14 models identified for temperature. Since the bias correction cannot be done with the SAFRAN reanalysis (which covers only France), we consider the ERA5 reanalysis [18] and use the CDF$-t$ univariate bias correction method [23] for SLP.

For comparison purposes with CMIP6, we extract the mean temperature over Ile-de-France for the ERA5 reanalysis (1950-2021) [18] from the climate explorer tool (https://climexp.knmi.nl/).

3.2 Heatwave identification

For each year, we consider moving 15-day periods between July 1st and August 31st. In each temperature time series (for each model, for each scenario), we determine the warmest yearly 15-day spell (TG15d). These values are reported in Figure 1. Each temperature value obviously corresponds to a different starting date. We then determine the first day of the moving 15-day hottest spells. Hence, rather than starting on a 26th of July (beginning of the 2024 Olympics), we start on the date determined by the warmest 15-day spell in July-August. This is close to the procedure for ensemble boosting simulations [24]. The paper then focuses on the most intense TG15d in 2001-2050.

3.3 Extreme Value Analysis

An upper bound estimate of the return value of a 15-day heatwave is inferred with the method of [25], based on Generalized Extreme Value (GEV) modelling [17]. A multi-model synthesis of non-stationary GEV parameters from each climate models is used as prior. A posterior is derived using Bayesian techniques based on SAFRAN reanalysis statistics, considered as a reference. This approach allows us to have a non-stationary GEV model covering the period 1850-2100 for each scenario, and constrained by the a reference reanalysis. With this procedure we obtain a statistical estimate of return levels associated to return periods of 100 years. We also compute 95% confidence intervals on the return level estimates.

3.4 Stochastic weather generator and importance sampling

We use the approach of [3], which emulates temperature variations with a stochastic weather generator (SWG) [26] based on analogs of atmospheric circulation. This corresponds to a Markov chain of temperature, with hidden states of the atmospheric circulation. For each day, we determine the 20 best analogs of SLP, by minimizing a Euclidean distance. There is an obvious trend in temperature in 2001-2050. But there is no apparent trend in the years of the 20 best SLP analogs. The reshuffling is done with weights that favor analogs with higher temperature over Ile-de-France. This corresponds to a procedure of *importance sampling* [3]. If the weights are uniform, this is equivalent to a normal emulator of temporal sequences [14]. Larger weights on higher temperatures help sampling the tail of the temperature distribution. We add a constraint on the calendar day, in order to emulate a seasonal cycle. We simulate 15-day sequences that are nudged towards high temperatures, starting on identified TG15d periods in 2001-2050, in CMIP6 model simulations.

The parameter that controls the weights towards high temperatures is $\alpha_T = 0.5$, which roughly corresponds to simulating centennial events [3].

3.5 Experimental set-up of simulations

We simulate heatwaves between 2001 and 2050, which are the five decades that roughly bracket 2024. We initiate heatwaves in this period from CMIP6 simulations, and evaluate the role of climate change in heatwave that "could have been", in historical and scenario configurations, with a constraint on the atmospheric circulation.

We compute SLP analogs of 1900-2100 in 1951-2000 (historical period) and 2001-2050 (scenario period). This is done for the four scenarios and 14 models. This helps sampling low frequency variability, since all models yield different ocean configurations.

The initial conditions of the SWG simulations are the first day of the warmest 15-day period (in July and August, TG15d), for each year (between 2001 and 2050), each model and each scenario. We simulate 200 trajectories for each initial condition. The paper focuses on simulations that are initiated on the warmest event in 2001-2050, in each model and each scenario. An illustration of such simulations with data from the IPSL model is provided in Figures 2 and 3. A synthesis with all 14 CMIP6 model data is shown in Figure 4.

4 Discussion

This study is an improvement over existing reports on the risk of heatwaves from climate projections [7], as we use state of the art bias correction methods, and a large set of CMIP6 simulations. We generalize the results of [3] by considering climate change. Rather than simulating many "normal" summers and extracting the hottest, our approach directly simulates many extremely hot summers. The computing efficiency makes this approach appealing: simulating 10^4 centennial heatwaves (just over France) with general circulation models would require more than 100 times the volume of available CMIP6 data.

This study is not a forecast for July-August 2024 in Paris, but a risk assessment of extreme heatwaves in a changing climate. Temperatures that exceed the 2003 record by $\approx 4°$C after 2020 in Ile-de-France are possible, although with a low probability (return time of ≈ 100 years). Model simulations suggest that such records could also be shattered in the 2020-2050 decades.

This study comes with caveats. Most selected initial conditions occur after 2020 in the CMIP6 simulations, due to the increase of temperature in the 2001-2050 period. This does not change the main message of the paper that the 2003 record can be broken, with the atmospheric circulation scenario that we identified, and which is possible in 1951-2000. No local physical processes are considered in these simulations. Soil moisture or atmospheric humidity could also be used to constrain analogs, but these quantities are not always available on a daily basis for the CMIP6 simulations we used. Taking such processes into account is possible with our approach, and could potentially enhance the heatwaves. Therefore, our estimates can be considered as lower bounds that are based mainly on atmospheric dynamics properties.

5 Conclusion

This paper takes information from 4 scenarios $\times$ 14 models = 56 extreme heatwaves of 15 days (TG15d) from CMIP6 simulations. We have produced an ensemble of $200 \times 56 \approx 10^4$ centennial heatwaves for the 2001-2050 decades. Those heatwaves exceed the 2003 record values in France and the record values in individual CMIP6 simulations.

Such climate events pose a serious health threat, especially for social events where crowds gather outdoors, like in the Olympic games. Those heat events seem to occur with anticyclonic conditions, leading to low surface winds, which enhances the health threat, as air pollutants are not dispersed [27]. The addition of a cut-off low that transports warm air from North Africa can increase the temperature in a short time.

Several studies have suggested that the most extreme events (e.g. the most extreme heatwaves at a given location) should yield the same general conditions [12, 28]. Those statements are based on *large deviation theory* that leads to an *instanton* or a *typical* extreme, which is the unique pathway leading to extremes of an observable in a dynamical system [29]. The similarity of SLP patterns during the most extreme heatwaves (from models and SWG simulations) hints at the validity of such a theory. Proving it requires specific climate model simulations with rare event algorithms [12, 13], which would require a major computing exercise.

The domain of application of our simulation approach obviously goes beyond the Paris Olympics in 2024 (or any major outdoors sports event in that region). It could be adapted to other regions of the world, where surface temperature is linked to the atmospheric circulation. Such an approach can be used to design so-called storylines of events [30, 31], for impact models or for communication on extreme events in a changing climate.

Supplementary information. This article has a supplementary file (list and references of CMIP6 models, SLP maps for 14 models).

Acknowledgments. We thank Soulivanh Thao for helping handling CMIP6 datasets.

Declarations

The authors acknowledge the support of the INSU-CNRS-LEFE-MANU grant (project DINCLIC: DF), the grant ANR-19-ERC7-0003 (BOREAS: DF) and the grant ANR-20-CE01-0008-01 (SAMPRACE: PY, CC), a CEA-ANDRA-EDF R& D grant (COSTO: PY), the "Explore2" French project (YR, MV), the French program LEFE (COESION: MV, DF). This work has received support from the European Union's Horizon 2020 research and innovation programme under grant agreement No. 101003469 (XAIDA: PY, DF, FP, MV). RN was supported by a doctoral grant from CEA.

The authors declare no conflict of interest.

Code availability: SWG code is available on github: https://github.com/pascalyiou/UNCLE-with-Analog-SWG. The bias correction code is available on github: https://github.com/yrobink/SBCK.

Data availability: ERA5 reanalysis temperature data is available from the Climate Explorer tool https://climexp.knmi.nl/start.cgi. CMIP6 data without bias corrections (temperature, SLP) is available from the Earth System Grid Federation (ESGF) node https://esgf-node.ipsl.upmc.fr/projects/cmip6-ipsl/. Bias corrected data (temperature, SLP), SLP analogs and SWG simulations are available upon request to the corresponding author (PY).

Authors contributions: PY designed the experiments. YR computed the bias CMIP6 correction and GEV estimates. All authors contributed to the writing of the manuscript.

References

[1] Schaer, C. & Jendritzky, G. Climate change: Hot news from summer 2003. *Nature* **432** (7017), 559–560 (2004). URL ⟨GotoISI⟩://000225433200023 .

[2] García-Herrera, R., Díaz, J., Trigo, R. M., Luterbacher, J. & Fischer, E. M. A review of the European summer heat wave of 2003. *Critical Reviews in Environmental Science and Technology* **40** (4), 267–306 (2010). ISBN: 1064-3389 Publisher: Taylor & Francis .

[3] Yiou, P. & Jézéquel, A. Simulation of extreme heat waves with empirical importance sampling. *Geosci. Model Dev.* **13** (2), 763–781 (2020).

URL https://www.geosci-model-dev.net/13/763/2020/. https://doi.org/10.5194/gmd-13-763-2020 .

[4] Eyring, V. *et al.* Overview of the Coupled Model Intercomparison Project Phase 6 (CMIP6) experimental design and organization. *Geoscientific Model Development* **9** (5), 1937–1958 (2016) .

[5] Kovats, R. S. & Hajat, S. Heat stress and public health: a critical review. *Annu. Rev. Public Health* **29**, 41–55 (2008). ISBN: 0163-7525 Publisher: Annual Reviews .

[6] Van Vliet, M. T., Sheffield, J., Wiberg, D. & Wood, E. F. Impacts of recent drought and warm years on water resources and electricity supply worldwide. *Environmental Research Letters* **11** (12), 124021 (2016). ISBN: 1748-9326 Publisher: IOP Publishing .

[7] Seneviratne, S. *et al.* in *Weather and Climate Extreme Events in a Changing Climate* (eds Masson-Delmotte, V. *et al.*) *Climate Change 2021: The Physical Science Basis. Contribution of Working Group I to the Sixth Assessment Report of the Intergovernmental Panel on Climate Change* 1513–1766 (Cambridge University Press, Cambridge, United Kingdom and New York, NY, USA, 2021). Type: Book Section.

[8] Watts, J. Olympic athletes and volunteers in Tokyo 'tortured' by hottest Games ever. *The Guardian* (2021). URL https://www.theguardian.com/environment/2021/aug/05/olympic-athletes-and-volunteers-in-tokyo-tortured-by-heat .

[9] Kakamu, T., Wada, K., Smith, D. R., Endo, S. & Fukushima, T. Preventing heat illness in the anticipated hot climate of the Tokyo 2020 Summer Olympic Games. *Environmental Health and Preventive Medicine* **22** (1), 68 (2017). URL https://doi.org/10.1186/s12199-017-0675-y. https://doi.org/10.1186/s12199-017-0675-y .

[10] Vanos, J. K. *et al.* Planning for spectator thermal comfort and health in the face of extreme heat: The Tokyo 2020 Olympic marathons. *Science of The Total Environment* **657**, 904–917 (2019). URL https://www.sciencedirect.com/science/article/pii/S0048969718348022. https://doi.org/https://doi.org/10.1016/j.scitotenv.2018.11.447 .

[11] National Academies of Sciences Engineering and Medicine (ed.) *Attribution of Extreme Weather Events in the Context of Climate Change* (The National Academies Press, Washington, DC, 2016). URL www.nap.edu/catalog/21852/attribution-of-extreme-weather-events-in-the-context-of-climate-change.

[12] Ragone, F., Wouters, J. & Bouchet, F. Computation of extreme heat waves in climate models using a large deviation algorithm. *Proc. Nat. Acad. Sci.* **115** (1), 24–29 (2018). ISBN: 0027-8424 Publisher: National Acad Sciences .

[13] Ragone, F. & Bouchet, F. Rare event algorithm study of extreme warm summers and heatwaves over Europe. *Geophys. Res. Lett.* **48** (12), e2020GL091197 (2021). https://doi.org/https://doi.org/10.1029/2020GL091197, iSBN: 0094-8276 Publisher: Wiley Online Library .

[14] Yiou, P. AnaWEGE: a weather generator based on analogues of atmospheric circulation. *Geoscientific Model Development* **7** (2), 531–543 (2014). URL http://www.geosci-model-dev.net/7/531/2014/. https://doi.org/10.5194/gmd-7-531-2014 .

[15] Yiou, P. *et al.* Analyses of the Northern European summer heatwave of 2018. *Bulletin of the American Meteorological Society* **101** (1), S35–S40 (2020) .

[16] Vrac, M. & Thao, S. R 2 D 2 v2. 0: accounting for temporal dependences in multivariate bias correction via analogue rank resampling. *Geoscientific Model Development* **13** (11), 5367–5387 (2020). ISBN: 1991-959X Publisher: Copernicus GmbH .

[17] Coles, S. *An introduction to statistical modeling of extreme values* Springer series in statistics (Springer, London, New York, 2001).

[18] Hersbach, H. *et al.* The ERA5 global reanalysis. *Quat. J. Roy. Met. Soc.* **146** (730), 1999–2049 (2020). ISBN: 0035-9009 Publisher: Wiley Online Library .

[19] Quesada, B., Vautard, R., Yiou, P., Hirschi, M. & Seneviratne, S. I. Asymmetric European summer heat predictability from wet and dry southern winters and springs. *Nature Climate Change* **2** (10), 736–741 (2012). https://doi.org/Doi10.1038/Nclimate1536 .

[20] Mueller, B. & Seneviratne, S. Hot days induced by precipitation deficits at the global scale. *Proc. Natl. Acad. Sci. USA* doi:10.1073/pnas.1204330109 (2012). https://doi.org/10.1073/pnas.1204330109 .

[21] Riahi, K. *et al.* The Shared Socioeconomic Pathways and their energy, land use, and greenhouse gas emissions implications: An overview. *Global environmental change* **42**, 153–168 (2017). ISBN: 0959-3780 Publisher: Elsevier .

[22] Quintana-Segui, P. *et al.* Analysis of near-surface atmospheric variables: Validation of the SAFRAN analysis over France. *Journal of applied*

meteorology and climatology **47** (1), 92–107 (2008). ISBN: 1558-8432 .

[23] Michelangeli, P.-A., Vrac, M. & Loukos, H. Probabilistic downscaling approaches: Application to wind cumulative distribution functions. *Geophysical Research Letters* **36** (11) (2009) .

[24] Gessner, C., Fischer, E. M., Beyerle, U. & Knutti, R. Very rare heat extremes: quantifying and understanding using ensemble reinitialization. *Journal of Climate* **34** (16), 6619–6634 (2021). ISBN: 0894-8755 .

[25] Robin, Y. & Ribes, A. Nonstationary extreme value analysis for event attribution combining climate models and observations. *Advances in Statistical Climatology, Meteorology and Oceanography* **6** (2), 205–221 (2020). ISBN: 2364-3579 Publisher: Copernicus GmbH .

[26] Ailliot, P., Allard, D., Monbet, V. & Naveau, P. Stochastic weather generators: an overview of weather type models. *Journal de la Société Française de Statistique* **156** (1), 101–113 (2015) .

[27] Pirard, P. *et al.* Summary of the mortality impact assessment of the 2003 heat wave in France. *Eurosurveillance* **10** (7), 7–8 (2005). ISBN: 1560-7917 Publisher: European Centre for Disease Prevention and Control .

[28] Gálfi, V. M., Lucarini, V. & Wouters, J. A large deviation theory-based analysis of heat waves and cold spells in a simplified model of the general circulation of the atmosphere. *Journal of Statistical Mechanics: Theory and Experiment* **2019** (3), 033404 (2019). ISBN: 1742-5468 Publisher: IOP Publishing .

[29] Lucarini, V., Galfi, V. M., Messori, G. & Riboldi, J. Typicality of the 2021 Western North America Summer Heatwave. *arXiv preprint arXiv:2206.06197* (2022) .

[30] Shepherd, T. G. Storyline approach to the construction of regional climate change information. *Proceedings of the Royal Society A* **475** (2225), 20190013 (2019) .

[31] Sillmann, J. *et al.* Event-Based Storylines to Address Climate Risk. *Earth's Future* **9** (2), e2020EF001783 (2021). https://doi.org/https://doi.org/10.1029/2020EF001783 .